Materials and Structures (2022) 55:181
https://doi.org/10.1617/s11527-022-02019-2

ORIGINAL ARTICLE

Evaluation of zero-stress temperature and cracking temperature of high performance concrete at early ages

Liang Li · Arosha Dabarera · Vinh Dao

Received: 10 January 2022 / Accepted: 11 April 2022 / Published online: 19 August 2022

Abstract Assessing the risk of cracking of high performance concrete induced by restrained volume changes from early ages is of considerable significance. To estimate and control such cracking risk of high performance concrete, two characteristic temperatures, namely zero-stress temperature (T_z) and cracking temperature (T_x) are crucial. In this study, the two temperatures are investigated in-depth by both theoretical analysis and experimental studies. For predicting the evolutions of T_z and T_x from early ages, rigorous yet practical models are proposed, which crucially take the visco-elastic behaviour of concrete into account. The reliability and predictive capability of the proposed models are demonstrated through a series of comparisons between the predicted and the measured results. Based on the predicted T_z and T_x profiles, practical thermal control criteria for preventing concrete from cracking caused by restrained strain are put forward. In principle, the actual temperature (T) of concrete should be kept higher than both T_z and T_x to properly maintain the stress induced by restrained strain in compression at early ages. If T becomes lower than T_z and reduces continuously, the lower the value of T, the higher the risk of cracking of concrete induced by restrained strain. As a consequence, once the value of T reaches or becomes lower than T_x, cracking is highly likely to occur. For a given actual temperature condition, lowering T_z and T_x can mitigate the risk of the cracking of concrete. Finally, effective measures for such lowering of T_z and T_x are also proposed.

Keywords Early-age concrete · Zero-stress temperature · Cracking temperature · Time-zero temperature · Restrained strain · Cracking risk

L. Li · A. Dabarera · V. Dao (✉)
School of Civil Engineering, The University of Queensland, Brisbane, Australia
e-mail: v.dao@uq.edu.au

L. Li
Department of Civil and Architectural Engineering, Aarhus University, Aarhus, Denmark

1 Introduction

Due to the release of hydration heat and the thermal interaction with the ambient environment after mixing, high performance concrete tends to experience considerable initial temperature rise and associated thermal expansion (see Fig. 1a and b). Then, as the hydration reaction slows down and the loss of hydration heat plays the dominant role, a cooling process commences and a corresponding thermal contraction happens [1]. In fact, besides thermal strain, considerable autogenous and drying shrinkage often take place simultaneously at early ages [2–6]. Since concrete structures are always subjected to a certain level of external restraint in practice, stress due

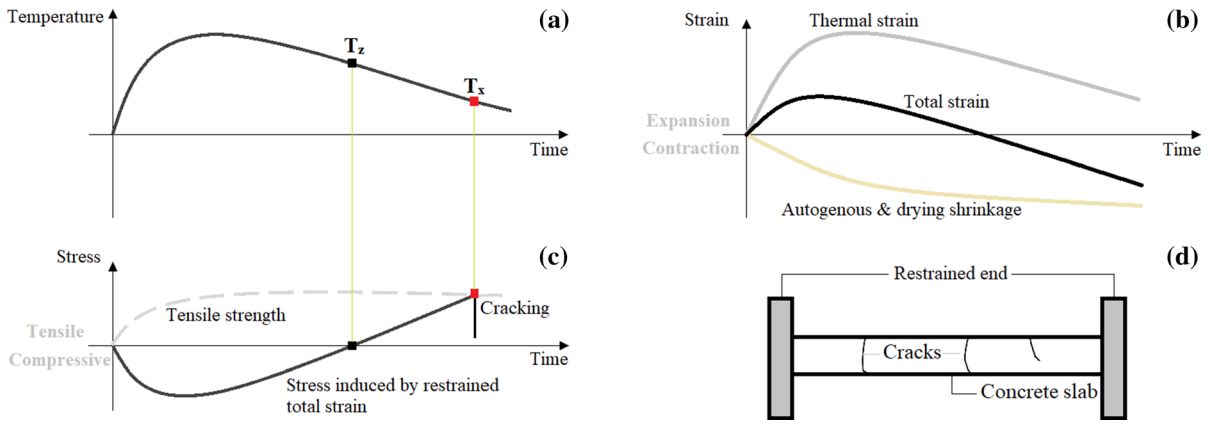

Fig. 1 Schematic diagram of the build-up of stress induced by the restrained volume changes of high performance concrete after setting

to restrained strain tends to occur. For an example of a thin concrete slab with external restraint (see Fig. 1d): as the total strain including thermal strain, autogenous shrinkage, and drying shrinkage expands at an initial stage (Fig. 1b), residual compressive stress evolves after creep relaxation, as shown in Fig. 1c. Subsequently, as the total strain shrinks, the residual compressive stress reduces and transfers into tensile stress progressively. As long as the tensile stress reaches the tensile strength of concrete, early-age cracking is the result (see Fig. 1d). According to [7–10], the concrete temperatures corresponding to the zero stress and the cracking stress are the zero-stress temperature (T_z) and the cracking temperature (T_x), as marked in Fig. 1a. The two feature temperatures are of significant importance to carry out a holistic study on the cracking risk of early-age concrete induced by restrained strain.

While measurements of T_z and T_x of early-age concrete had been reported in the past studies [7–12], there remain no appropriate numerical models for the two temperatures. In this paper, an attempt has been made to model the evolutions of the two temperatures at early ages based on substantial previous studies performed by the authors [5, 10, 13]. Both the theoretical basis and practical significance of predicting T_z and T_x were presented and justified. Moreover, effective and practical measures for minimizing the risk of cracking of concrete caused by restrained strain are also discussed.

2 Theoretical basis

To determine the stress induced by externally restrained strain, a phenomenological model based on the elastic stress–strain response of concrete has been proposed in [14], as given below:

$$\begin{aligned}\boldsymbol{\sigma}_{\mathrm{tot}}(t) &= E_e(t)\cdot R_{\mathrm{res}}(t)\cdot \boldsymbol{\varepsilon}_{\mathrm{tot}}(t)\\ &= E_e(t)\cdot R_{\mathrm{res}}(t)\cdot \underbrace{\left(\boldsymbol{\varepsilon}_{\mathrm{th}}(t)+\boldsymbol{\varepsilon}_{\mathrm{as}}(t)+\boldsymbol{\varepsilon}_d(t)\right)}_{\text{restraint-free total strain}}\end{aligned} \quad (1)$$

where t is the age of concrete, $\boldsymbol{\sigma}_{\mathrm{tot}}$ is the total stress induced by the restrained total strain ($R_{\mathrm{res}}\,\boldsymbol{\varepsilon}_{\mathrm{tot}}$), and R_{res} is the degree of restraint. $\boldsymbol{\varepsilon}_{\mathrm{th}}$, $\boldsymbol{\varepsilon}_{as}$, and $\boldsymbol{\varepsilon}_d$ are free thermal strain, autogenous and drying shrinkage of concrete, respectively. For the strains in Eq. (1), contraction is defined as positive, and expansion as negative. E_e is the effective elastic modulus that takes aging and stress relaxation (or creep) of early-age concrete into account. According to [15], the effective elastic modulus can then be expressed as:

$$E_e(t) = \frac{E(t)}{1+\beta(t)\varphi(t)} \quad (2)$$

where $E(t)$ is the elastic modulus, $\beta(t)$ is an aging coefficient (of between 0.6 and 1.0) [16], and $\varphi(t)$ is the creep coefficient. According to the authors' research in [17, 18], $\varphi(t)$ of early-age concrete can be approximated using a revised MC2010 creep model.

Although Eq. (1) is proposed primarily for a 1D configuration, the equation is valuable for assessing the stress of concrete induced by restrained strain in reality. Generally, combined with the finite element

method, Eq. (1) can be applied to model the stresses in 3D concrete members with complex geometries [19]. For those concrete slabs, beams, and columns which can be simplified as a 1D configuration, the equation can be used directly. In terms of the potential defect of Eq. (1), further discussion can be found in Sects. 4 and 5.

2.1 Zero-stress temperature

For fresh concrete, despite considerable volume change before setting (or the time-zero) [5, 20, 21], no stress due to restrained strain appears. After time-zero, concrete starts to behave like a solid (with $E_e > 0$) and enables stress transfer. According to Eq. (1), to maintain $\boldsymbol{\sigma}_{\text{tot}}$ at negligible levels, the restraint-free $\boldsymbol{\varepsilon}_{\text{tot}}$ should be kept as close to zero as practicable since R_{res} is generally non-zero. On that basis, the fictitious temperature profile (T_z) that keeps $\boldsymbol{\varepsilon}_{\text{tot}}$ equal to zero (and thereby always zeros $\boldsymbol{\sigma}_{\text{tot}}$) can be expressed as

$$\boldsymbol{\varepsilon}_{\text{as}}(t) + \boldsymbol{\varepsilon}_d(t) + \underbrace{\alpha_{\text{CTE}}(t) \cdot (T_0(t_0) - T_z(t))}_{\boldsymbol{\varepsilon}_{\text{th}}(t)} = 0 \tag{3}$$

where $T_z(t)$ is the zero-stress temperature, $\alpha_{CTE}(t)$ is the coefficient of thermal expansion (CTE). $T_0(t_0)$ is the initial reference temperature (or namely, time-zero temperature) for thermal stress and strain analysis of high performance concrete, which refers to the temperature at time-zero (t_0) [22]. In this study, the time-zero (t_0) of fresh concrete is defined as the time point when concrete materials form a stable solid skeleton to develop tensile and compressive stresses [5].

Rearranging Eq. (3), $T_z(t)$ can be determined by

$$T_z(t) = T_0(t_0) + \frac{\boldsymbol{\varepsilon}_{\text{as}}(t) + \boldsymbol{\varepsilon}_d(t)}{\alpha_{\text{CTE}}(t)} \tag{4}$$

2.2 Cracking temperature

Through the analysis above, the improved model to determine the total stress (Eq. (1)) induced by restrained total strain under an actual temperature profile (T) can be presented as [10]:

$$\boldsymbol{\sigma}_{\text{tot}}(t) = E_e(t) \cdot R_{\text{res}}(t) \cdot \alpha_{\text{CTE}}(t) \cdot (T_Z(t) - T(t)) \tag{5}$$

It is clear that as long as the actual temperature (T) and T_z are the same, $\boldsymbol{\sigma}_{tot}$ is zero. When T is higher than T_z, $\boldsymbol{\varepsilon}_{\text{tot}}$ is expansive, causing compressive stress. On the contrary, if T is lower than T_z, then $\boldsymbol{\varepsilon}_{tot}$ is contractive, resulting in tensile stress. Once the tensile stress reaches the actual tensile carrying capacity ($k \cdot f_t$) of early-age concrete, cracking induced by restrained strain happens. Given the cracking of concrete initiates when T reaches the cracking temperature T_x, then

$$\begin{aligned}\boldsymbol{\sigma}_{\text{tot}}(t) &= E_e(t) \cdot R_{\text{res}}(t) \cdot \alpha_{\text{CTE}}(t) \cdot (T_z(t) - T_x(t)) \\ &= k \cdot f_t(t)\end{aligned} \tag{6}$$

where, f_t is the tensile strength of concrete samples measured in accordance with relevant standards, and k is a coefficient for approximating the actual in-situ tensile carrying capacity of concrete. Typically, k is between 0.6 and 0.8 [23–25].

From Eq. (6), the cracking temperature (T_x) can be expressed as:

$$T_x(t) = T_z(t) - \frac{k \cdot f_t(t)}{E_e(t) \cdot R_{\text{res}}(t) \cdot \alpha_{\text{CTE}}(t)} \tag{7}$$

Theoretically, $T_x(t)$ represents a critical temperature profile of concrete that designates conditions at which the initiation of cracking takes place. Once the actual concrete temperature becomes lower than $T_x(t)$, cracks propagate. Besides, it should be noted that the obtained T_z and T_x profiles of concrete (Eqs. (4) and (7)) are both essentially temperature-dependent, due mainly to the effects of actual temperature on the evolutions of autogenous shrinkage, effective elastic modulus, CTE, and tensile strength at early ages [26–28]. This indicates that the evolutions of $T_z(t)$ and $T_x(t)$ of young concrete can be a function of equivalent age.

3 Evolutions of T_z and T_x profiles of concrete at early ages

3.1 Concrete mix

Following the authors' previous studies [5, 10, 17, 29], a concrete mix with water-to-binder ratio (w/b) of 0.25 (see Table 1) was studied to demonstrate the determination and evolution of T_z and T_x profiles in this paper.

Table 1 Mix compositions of concrete with w/b of 0.25 (kg/m^3)

Ordinary Portland cement	Fly ash	Silica fume	Water	10 mm aggregate	Coarse sand	Fine sand
560	120	40	180	930	250	240

The 28-day compressive strength of the concrete is approximately 85.0 MPa. The oxide compositions of cementitious materials and particle sizes of aggregates used in the concrete mix can be found in Tables 2 and 3.

3.2 Key properties of concrete

All key parameters of the concrete mix used in the calculations of T_z and T_x can be found in [5], in which the autogenous shrinkage, CTE, elastic modulus, splitting tensile strength, and time-zero are reported. In this study, these physical properties of young concrete are modelled using equivalent age (or maturity). According to [30–32], the equivalent age is calculated by Eq. (8).

$$t_e = \int_0^t \left[\exp\frac{-E_a}{R}\left(\frac{1}{T(t)} - \frac{1}{T_{\text{ref}}}\right)\right] \mathrm{d}t \tag{8}$$

where E_a is the activation energy (J/mol), $T(t)$ is the temperature history of concrete, R is the ideal gas constant (8.3 J/(mol·K)), and T_{ref} is the reference temperature (293.0 K).

In this study, E_a is taken as 30.0 kJ/mol, as recommended for cementitious pastes containing fly ash and silica fume in [33]. Improved empirical models for simulating each key property of young concrete as a function of equivalent age are given below.

3.2.1 Autogenous shrinkage

Figure 2 shows the development of autogenous shrinkage of the concrete at early ages. To match the measured autogenous shrinkage, a modified empirical model (Eq. (9)) recommended in the CEB-FIP standard [34] and Eurocode 2 [35] is used, as follows:

$$\varepsilon_{\text{as}}(t_e) = \varepsilon^*_{\text{as}}\left(1 - \exp\left(-0.2(t_e - t_0)^{0.5}\right)\right) \tag{9}$$

where $\varepsilon^*_{\text{as}}$ is the estimated ultimate autogenous shrinkage, and t_e is the equivalent age in days. By fitting the test data using a nonlinear regression method, $\varepsilon^*_{\text{as}}$ and t_0 can be determined and equal -390×10^{-6} m/m and 8.5 h ($\sim$ 0.35 d), respectively.

3.2.2 Coefficient of thermal expansion

The evolution of the CTE of early-age concrete (see Fig. 3) is modelled by the following equation:

$$\alpha(t_e) = \alpha^*_{\text{CTE}}\left(1 - \exp\left(-a(t_e - t_0)^b\right)\right) \tag{10}$$

where, α^*_{CTE} is the estimated ultimate CTE of concrete (taken as 12.0×10^{-6}/°C). a and b are fitting parameters (0.20 and 0.41, respectively).

Table 2 Oxide compositions of cement, fly ash, and silica fume (by mass, %)

	Ordinary Portland cement	Fly ash	Silica fume
CaO	63.9	3.80	–
SiO_2	19.5	59.4	89.9
Al_2O_3	5.40	20.4	–
SO_3	2.64	0.20	0.84
Fe_2O_3	2.83	10.9	–
MgO	1.40	1.50	–
Na_2O	0.32	0.67	0.11
K_2O	0.42	1.42	0.23
Loss on ignition	3.11	0.70	3.80

Table 3 Particle size distribution of sands and 10 mm aggregate

Sieve size (mm)		14.00	9.50	4.75	2.36	1.18	0.60	0.30	0.15	0.075
Passing rate (%)	Fine sand	100	100	97.4	83.1	68.7	44.7	16.5	4.5	1.0
	Coarse sand	100	100	99.5	75.5	46.3	26.9	14.1	7.3	3.3
	10 mm aggregate	100	86.8	6.8	2.0	1.7	1.5	1.3	1.1	0.4

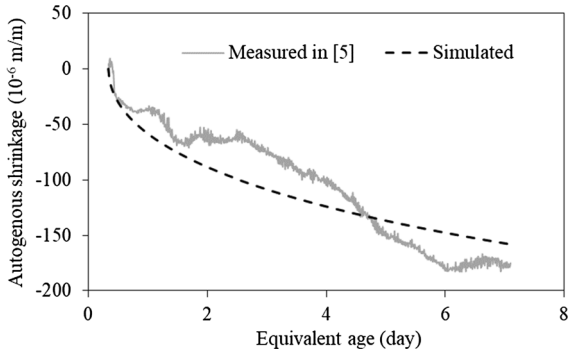

Fig. 2 Autogenous shrinkage of early-age concrete as a function of equivalent age

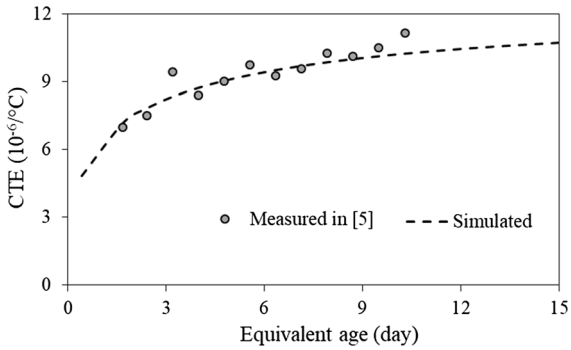

Fig. 3 Evolution of the CTE of early-age concrete

3.2.3 Elastic modulus

A revised model (Eq. (11)) drawn from the Eurocode 2 [35] is applied to simulate the development of the elastic modulus of early-age concrete measured in [5], as shown in Fig. 4. Combing Eqs. (11) and (2), the effective elastic modlus can be obtained.

$$E(t_e) = E^* \cdot \exp\left\{ s \cdot \left[1 - \left(\frac{28}{t_e - t_0} \right)^n \right] \right\} \quad (11)$$

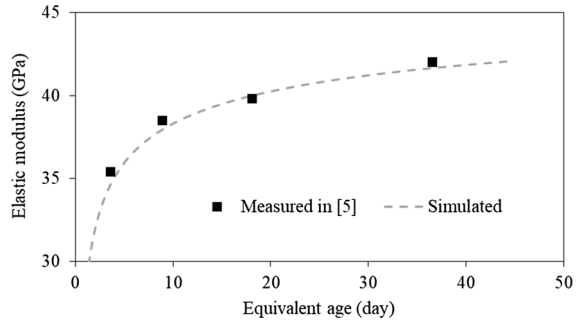

Fig. 4 Elastic modulus of early-age concrete as a function of equivalent age

where, E^* is the ultimate elastic modulus of concrete ($\sim$ 48.0 GPa), and s and n are fitting coefficients (0.018 and 0.32, respectively).

3.2.4 Tensile strength

Figure 5 presents the splitting tensile strength of the concrete measured in [5] and modelled by Eq. (12). Based on the splitting tensile strength, the direct tensile strength of concrete can be estimated by multiplying by a conversion factor of 0.9 [35, 36].

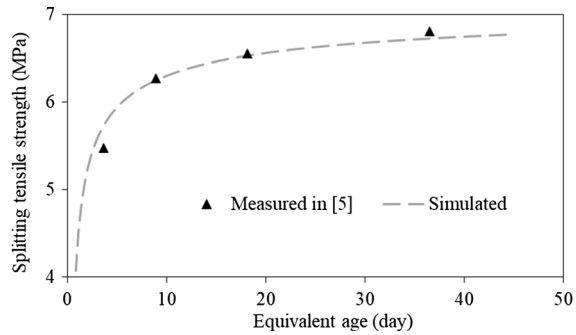

Fig. 5 Development of splitting tensile strength of early-age concrete

$$f(t_e) = f_t^* \cdot \exp\left\{p \cdot \left[1 - \left(\frac{28}{t_e - t_0}\right)^q\right]\right\} \quad (12)$$

where, f_t^* is the ultimate splitting tensile strength of concrete. p and q are fitting coefficients. In this study, f_t^*, p, and q are 7.1 MPa, 0.015, and 0.5, respectively.

3.3 Results and discussion

Inputting those key properties presented above into Eqs. (4) and (7), the T_z and T_x profiles of the concrete with w/b of 0.25 were obtained (see Fig. 6). For simplicity, drying shrinkage was neglected in the calculation, due to the negligible shrinkage of the concrete under sealed conditions in [5]. The temperature of concrete at the time-zero was assumed at $\sim$ 20 °C, and the degree of restraint was deemed as 1.0. In Fig. 6, it can be observed that the obtained T_z profile increases over time, resulting mainly from the development of autogenous shrinkage of concrete at early ages. Different from the evolution of T_z, the determined T_x profile firstly decreases dramatically and then increases gradually. This may be due to the combined effect of the fast evolution of tensile strength and the low effective elastic modulus and CTE at early ages (as presented by Eq. (7)).

To form an in-depth understanding of the practical significance of the obtained T_z and T_x profiles, a random actual temperature profile (T) is assumed in Fig. 6. It can be observed that T is split into three areas by T_z and T_x profiles:

Area A: T is larger than T_z, indicating the total stress of concrete induced by restrained strain is compressive (see Eq. (5)). The higher the value of T, the larger the compressive stress;

Area B: T is lower than T_z but remains higher than T_x, meaning that the compressive stress induced by restrained strain has transferred into tensile stress. The lower the value of T, the larger the tensile stress, and the higher the cracking risk of concrete;

Area C: T is lower than T_x, implying that the tensile stress induced by restrained strain exceeds the tensile carrying capacity of concrete. Cracks appear and propagate.

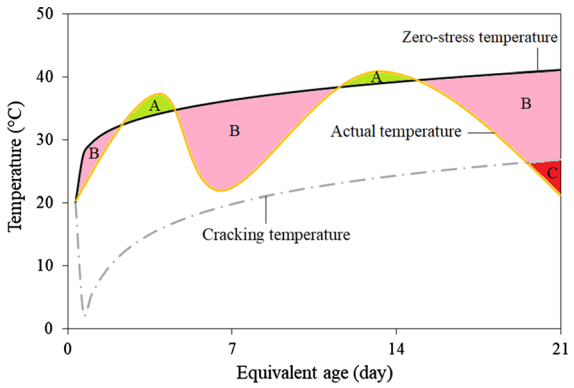

Fig. 6 Evolutions of T_z and T_x of early-age concrete as a function of equivalent age

From the analysis above, it is clear that for a given actual temperature profile, lowering T_z and T_x is of considerable significance for mitigating the risk of early-age cracking [9]. According to Eqs. (4) and (7), under a specified degree of restraint, minimizing the magnitude of autogenous and drying shrinkage or reducing the time-zero temperature (T_0) can lower both T_z and T_x. Besides, increasing tensile strength or decreasing effective elastic modulus & CTE can reduce T_x exclusively. In practice, modifying the deformational and mechanical properties of the concrete with a given mix design is challenging. Therefore, the most convenient measure for lowering T_z and T_x is to decrease T_0, which can be practically achieved by a wide range of temperature control measures [37]. For example, concrete mixing and casting are scheduled at night or in cool weather. Or, aggregates and water used for producing concrete are cooled before mixing. In previous studies, those temperature control measures are proposed mainly for limiting the peaking temperature of concrete or mitigating the temperature rise induced by hydration heat at early ages. In this study, the potential significance of reducing T_0 for lowering T_z, T_x, and thereby associated cracking risk of concrete is highlighted.

4 Assessment of the proposed T_z model

In [4, 38, 39], the stress of early-age concrete caused by restrained thermal strain and autogenous shrinkage (excluding drying shrinkage) was studied, as shown in Figs. 7, 8, 9. Combining the measured temperature and shrinkage data in [4, 38, 39] and Eq. (4), the T_z profile of each concrete mix was determined, see Figs. 7, 8, 9. Because of the lack of data for maturity transformation, the obtained T_z profiles were described as a

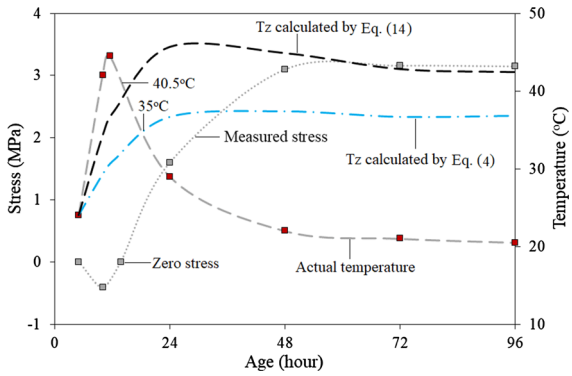

Fig. 7 Measured and calculated T_z of early-age concrete (w/b of 0.34), adapted from [4]

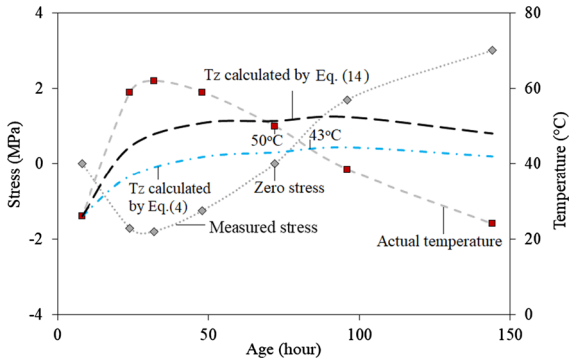

Fig. 8 Measured and calculated T_z of early-age concrete (w/b of 0.40), adapted from [38]

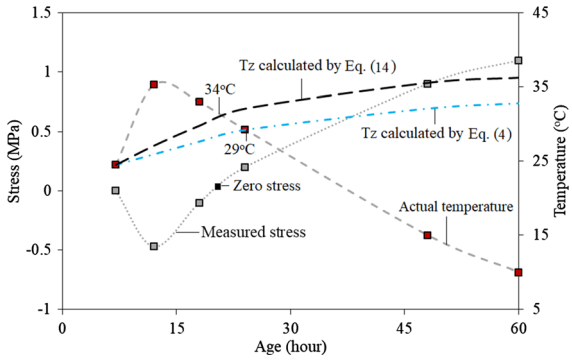

Fig. 9 Measured and calculated T_z of early-age concrete (w/b of 0.35), adapted from [39]

function of age. Besides, Eq. (10) was used to approximate the evolution of the CTE at early ages.

In Figs. 7, 8, and 9, the characteristic T_z points determined by the cross-over point of the actual temperature profile and the calculated T_z profile are ~ 35.0, ~ 43.0, and ~ 29.0 °C, respectively. But, the realistically measured T_z points, corresponding to the measured zero stress in Fig. 7 – 9 are ~ 40.5, ~ 50.0, and ~ 34.0 °C, respectively. The determined T_z results seem to be always lower than those correspondingly measured values, which may be due mainly to neglecting the visco-elastic response of concrete in Eq. (1). As stressed in Sect. 2, Eq. (1) is essentially built on the assumption of elastic stress–strain behaviour of concrete. However, under sustained loads, the actual stress–strain response of concrete is non-elastic [40–43], due to the existence of non-recoverable creep component (or plastic strain).

5 Finalized T_z and T_x models

To take plastic strains (ε_p) of early-age concrete under sustained loads into account, the original T_z model (Eq. (4)) can be revised as follows

$$T_z(t) = T_0(t_0) + \frac{\varepsilon_{\mathrm{as}}(t) + \varepsilon_d(t) + \varepsilon_p(t)}{\alpha_{\mathrm{CTE}}(t)} \tag{13}$$

However, ε_p as an input parameter in Eq. (13) is hard to be determined or approximated. For convenience, Eq. (13) can be further improved by introducing a coefficient γ instead of ε_p. The modified T_z model is expressed as

$$T_z(t) = T_0(t_0) + \frac{\varepsilon_{as}(t) + \varepsilon_d(t)}{\alpha_{\mathrm{CTE}}(t)} \cdot \gamma(t) \tag{14}$$

where, $\gamma(t)$ is a conversion coefficient drawn from the B3 model in which it represents the visco-elastic compliance of concrete [44–46], as given below

$$\gamma(t) = \gamma_0\left(1 + \exp\left(-g(t - t_0)^h\right)\right) \tag{15}$$

where, γ_0, g, and h are fitting parameters.

Qualitatively, with the strength and elastic modulus developing from very early ages, the non-elastic response of concrete tends to diminish [40–43]. Accordingly, the conversion coefficient (γ) reduces over time. Using nonlinear regression analysis to achieve a good fitting between the measured and predicted T_z in [4, 38, 39], γ_0, g, and h are set to 1.25, 0.30, and 0.41, respectively (as shown in Figs. 7, 8, 9).

To further examine the applicability of the improved T_z model with the determined γ, a comparison between the measured and predicted T_z results of the concrete mix with w/b ratio of 0.25 (see Table 1) is

performed. In [10], the authors measured the T_z of the concrete in accordance with modified uniaxial restrained shrinkage tests, using a Temperature Stress Testing Machine [27, 47]. For obtaining multiple zero-stress temperatures, a fluctuating temperature profile was imposed on a concrete specimen under fully restrained conditions from an age of 3 days onwards, as plotted in Fig. 10. In parallel, the total strain of another specimen under the same temperature history but restraint-free conditions was also measured. The two test specimens were both fully sealed by adhesive foil tape to achieve negligible moisture interaction between concrete and ambient environment. Autogenous shrinkage (AS, see Fig. 10) was obtained by subtracting thermal strain from the free total strain, as reported in [27]. Based on the determined autogenous shrinkage and CTE in [10], the T_z profile of the concrete was calculated by Eqs. (4) and (14), respectively. In Fig. 10, it can be observed that the T_z profile determined by Eq. (14) matches those measured T_z points better than the other profile, which demonstrates the suitability of the proposed conversion coefficient γ (Eq. (15)). To sum up, Eq. (15) appears to be proper for approximating the visco-elastic behaviour of early-age concrete with w/b between 0.25 and 0.40 (as shown in Figs. 7, 8, 9, 10). However, it should be noted that those fitting coefficients (γ_0, g, and h) may vary for other concrete mixes with significantly low or high w/b.

In addition, combining Eq. (14) with Eq. (7), the revised T_x model with visco-elastic behaviour taken into account can be obtained. To examine the predictive capability of the T_x model, further data analysis is carried out. In [9], the stress of concrete mix with w/b of 0.385 induced by restrained strain is experimentally measured, using a rigid cracking frame. As shown in Fig. 11, the measured stress reaches zero at $\sim$ 30 h, and the cracking of concrete takes place at $\sim$ 105 h. Correspondingly, the T_z and T_x at $\sim$ 30 h and $\sim$ 105 h are $\sim$ 53.1 °C and $\sim$ 23.0 °C, respectively. Due to the absence of the measured autogenous shrinkage in [9], it is challenging to obtain a precise T_z profile of the concrete. The T_z profile given in Fig. 11 was approximated according to Eq. (14) and the measured T_z at $\sim$ 30 h. On that basis, the T_x profile of concrete from 24 h onwards was estimated by Eq. (7). In the determination of T_x, a constant basic creep coefficient of 2.0 was used to transfer the measured elastic modulus in [9] into effective elastic modulus (via Eq. (2)). Such value of basic creep coefficient is recommended by the Australian Standard (AS3600—2018) [48] for concrete with 28-day compressive strength of over 60 MPa.

In Fig. 11, the calculated T_x profile shows an overall rising trend at early ages, which is consistent with the estimated T_x profile in Fig. 6. From 24 h to $\sim$ 103 h, the actual concrete temperature (T) is always higher than the value of the estimated T_x, indicating no cracking occurs. As both T and T_x profiles evolve over time, a cross-over between T and T_x occurs at $\sim$ 103 h, indicating that cracking takes place. The temperature at 103 h can therefore be

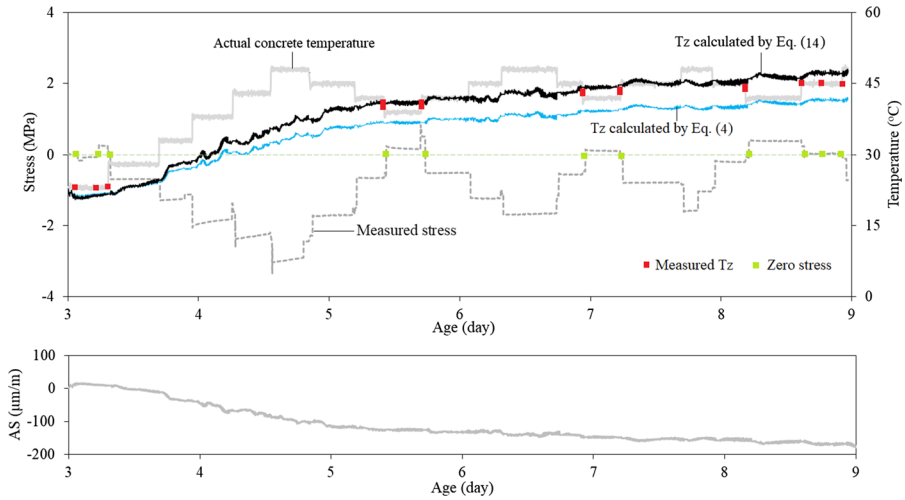

Fig. 10 Measured and calculated T_z of early-age concrete (w/b of 0.25), adapted from [10]

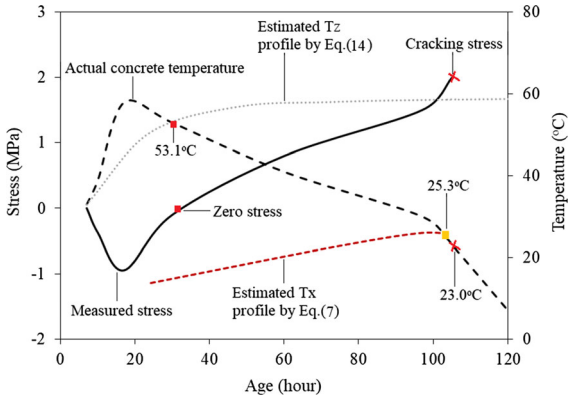

Fig. 11 T_z and T_x of early-age concrete (w/b of 0.385), adapted from [9]

regarded as the estimated T_x value ($\sim$ 25.3 °C) under the given temperature condition in [9]. Compared to the realistically measured T_x ($\sim$ 23.0 °C) in [9], the predicted outcome ($\sim$ 25.3 °C) appears to be quite acceptable. The prediction error is approximately 10% ($\frac{25.3-23}{23} \times 100\%$). Such good agreement between the predicted and measured T_x points again demonstrates the validity of the proposed T_z and T_x models in this study.

6 Conclusions

In this study, the zero-stress temperature (T_z) and the cracking temperature (T_x) associated with the volume change of high performance concrete are investigated in-depth. The key contributions and findings of the research can be summarized as follows:

- Both the practical significance and the theoretical basis for obtaining continuous T_z and T_x profiles of high performance concrete from very early ages are clarified. Unique models with the visco-elastic behaviour of concrete taken into account are proposed for predicting the evolutions of T_z and T_x profiles at early ages. The predictive capability of the T_z and T_x models is demonstrated through a series of comparisons between the predicted and the measured results;
- Based on the determined T_z and T_x profiles, practical thermal control criteria for assessing and mitigating the risk of cracking of concrete induced by restrained volume change are proposed and justified. Ideally, the actual temperature of concrete (T) should be kept higher than both T_z and T_x in order to maintain the stress induced by restrained strain in compression. Once the value of T becomes lower than T_z, tensile stress caused by restrained strain develops. As the value of T continues to decrease, the tensile stress rapidly approaches the tensile carrying capacity of concrete. When T is equal to or lower than T_x, the risk of cracking becomes markedly high. To minimize such cracking risk, thermal control measures must be taken to (i) lower T_x and (ii) ensure T being kept always higher than T_x. For lowering T_z and T_x, in addition to mitigating the autogenous and drying shrinkage as well as increasing the tensile strength of early-age concrete, reducing the temperature of concrete at the time-zero is also beneficial.

Acknowledgements The authors gratefully acknowledge the financial support from the Australian Research Council (Discovery Projects Scheme, DP180103160). The authors thank Professor Pietro Lura (Empa, Switzerland) for his critical reading of the manuscript. The first author also acknowledges the financial support from the Danish Hydrocarbon Research and Technology Centre, Denmark.

Authors' contributions LL: Conceptualization, methodology, investigation, writing- original draft, writing—review & editing. AD: investigation, writing—review & editing. VD: conceptualization, methodology, supervision, project administration, funding acquisition, writing—review & editing.

Funding Open Access funding enabled and organized by CAUL and its Member Institutions. This study was funded by the Australia Research Council project (DP 180103160). The first author also acknowledges the financial support from the Danish Hydrocarbon Research and Technology Centre, Denmark.

Availability of data and materials Not applicable.

Code availability Not applicable.

Declarations

Competing interests The authors declare that they have no known competing financial interests or personal relationships that could have appeared to influence the work reported in this paper.

References

1. Benboudjema F, Carette J, Delsaute B et al (2018) Chapter 4 mechanical properties. In: Fairbairn EMR, Azenha M (eds) Thermal cracking of massive concrete structures: state of the art report of the RILEM Technical Committee 254-CMS. Springer, Berlin, pp 69–114
2. Mechtcherine V, Gorges M, Schroefl C et al (2014) Effect of internal curing by using superabsorbent polymers (SAP) on autogenous shrinkage and other properties of a high-performance fine-grained concrete: Results of a RILEM round-robin test. Mater Struct 47:541–562. https://doi.org/10.1617/s11527-013-0078-5
3. Jensen OM, Lura P (2006) Techniques and materials for internal water curing of concrete. Mater Struct 39:817–825. https://doi.org/10.1617/s11527-006-9136-6
4. Cusson D, Hoogeveen T (2008) Internal curing of high-performance concrete with pre-soaked fine lightweight aggregate for prevention of autogenous shrinkage cracking. Cem Concr Res 38:757–765. https://doi.org/10.1016/j.cemconres.2008.02.001
5. Li L, Dabarera AGP, Dao V (2020) Time-zero and deformational characteristics of high performance concrete with and without superabsorbent polymers at early ages. Constr Build Mater 264:120262. https://doi.org/10.1016/j.conbuildmat.2020.120262
6. Radlinska A, Pease B, Weiss J (2007) A preliminary numerical investigation on the influence of material variability in the early-age cracking behavior of restrained concrete. Mater Struct 40:375–386. https://doi.org/10.1617/s11527-006-9118-8
7. Yeon JH (2015) Implications of zero-stress temperature for the long-term behavior and performance of continuously reinforced concrete pavement. Constr Build Mater 91:94–101. https://doi.org/10.1016/j.conbuildmat.2015.05.043
8. Sok T, Kim YK, Lee SW (2020) Numerical approach to predict zero-stress temperature in concrete pavements. Constr Build Mater 262:120076. https://doi.org/10.1016/j.conbuildmat.2020.120076
9. Markandeya A, Shanahan N, Gunatilake DM et al (2018) Influence of slag composition on cracking potential of slag-portland cement concrete. Constr Build Mater 164:820–829. https://doi.org/10.1016/j.conbuildmat.2017.12.216
10. Dabarera A, Li L, Lura P, Dao V (2022) Assessing the zero-stress temperature in high performance concrete at early age. Cem Concr Compos 127:104384. https://doi.org/10.1016/j.cemconcomp.2021.104384
11. Springenschmid R (1994) Thermal cracking in concrete at early ages. EFN SPON, Germany
12. Xin J, Liu Y, Zhang G et al (2021) Comparison of thermal cracking potential evaluation criteria for mass concrete structures. Mater Struct 54:1–15. https://doi.org/10.1617/s11527-021-01840-5
13. Dao V, Nguyen D, Lura P (2014) Early-age thermal cracking in concrete structures - the role of zero-stress temperature? In: The 14th East Asia - pacific conference on structural engineering and construction, pp 692–698
14. Bjøntegaard Ø (2011) Basis for and practical approaches to stress calculations and crack risk estimation in hardening concrete structures – State of the art. SINTEF Building and Infrastructure
15. Bažant ZP (1972) Prediction of concrete creep effects using age-adjusted effective. J Am Concr Inst 69:212–217
16. Kovler K (1994) Testing system for determining the mechanical behaviour of early age concrete under restrained and free uniaxial shrinkage. Mater Struct 27:324–330. https://doi.org/10.1007/BF02473424
17. Dabarera A, Li L, Lura P, Dao V (2022) Experimental assessment and modelling of effective tensile elastic modulus in high performance concrete at early age. Constr Build Mater 319:126125. https://doi.org/10.1016/j.conbuildmat.2021.126125
18. Li L, Dabarera AGP, Dao V (2022) Basic tensile creep of concrete with and without superabsorbent polymers at early ages. Constr Build Mater 320:126180. https://doi.org/10.1016/j.conbuildmat.2021.126180
19. Maruyama I, Lura P (2019) Properties of early-age concrete relevant to cracking in massive concrete. Cem Concr Res 123:105770. https://doi.org/10.1016/j.cemconres.2019.05.015
20. Sant G, Dehadrai M, Bentz D, et al (2009) Detecting the fluid-to-solid transition in cement pastes. Concr Int 53–58
21. Huang H, Ye G (2017) Examining the "time-zero" of autogenous shrinkage in high/ultra-high performance cement pastes. Cem Concr Res 97:107–114. https://doi.org/10.1016/j.cemconres.2017.03.010
22. Shen D, Wang W, Liu J et al (2018) Influence of Barchip fiber on early-age cracking potential of high performance concrete under restrained condition. Constr Build Mater 187:118–130. https://doi.org/10.1016/j.conbuildmat.2018.07.121
23. Xin J, Zhang G, Liu Y et al (2018) Effect of temperature history and restraint degree on cracking behavior of early-age concrete. Constr Build Mater 192:381–390. https://doi.org/10.1016/j.conbuildmat.2018.10.066
24. Wei Y, Hansen W (2013) Early-age strain-stress relationship and cracking behavior of slag cement mixtures subject to constant uniaxial restraint. Constr Build Mater 49:635–642. https://doi.org/10.1016/j.conbuildmat.2013.08.061
25. Shen D, Jiang J, Shen J et al (2016) Influence of curing temperature on autogenous shrinkage and cracking resistance of high-performance concrete at an early age. Constr Build Mater 103:67–76. https://doi.org/10.1016/j.conbuildmat.2015.11.039
26. Lura P, Van Breugel K, Maruyama I (2001) Effect of curing temperature and type of cement on early-age shrinkage of

high-performance concrete. Cem Concr Res 31:1867–1872. https://doi.org/10.1016/S0008-8846(01)00601-9
27. Li L, Dao V, Lura P (2021) Autogenous deformation and coefficient of thermal expansion of early-age concrete: initial outcomes of a study using a newly-developed temperature stress testing machine. Cem Concr Compos 119:103997. https://doi.org/10.1016/j.cemconcomp.2021.103997
28. Klausen AE, Kanstad T, Bjøntegaard Ø, Sellevold EJ (2018) The effect of realistic curing temperature on the strength and E-modulus of concrete. Mater Struct 51:1–14. https://doi.org/10.1617/s11527-018-1299-4
29. Dabarera A, Li L, Dao V (2021) Experimental evaluation and modelling of early-age basic tensile creep in high-performance concrete. Mater Struct 54:1–16. https://doi.org/10.1617/s11527-021-01722-w
30. Hansen PF, Pedersen EJ (1977) Maturity computer for controlled curing and hardening of concrete
31. De Schutter G (2004) Applicability of degree of hydration concept and maturity method for thermo-visco-elastic behaviour of early age concrete. Cem Concr Compos 26:437–443. https://doi.org/10.1016/S0958-9465(03)00067-2
32. Waller V, D'Aloïa L, Cussigh F, Lecrux S (2004) Using the maturity method in concrete cracking control at early ages. Cem Concr Compos 26:589–599. https://doi.org/10.1016/S0958-9465(03)00080-5
33. Poole JL, Riding KA, Folliard KJ, et al (2007) Methods for calculating activation energy for portland cement. ACI Mater J 104:86–94. https://doi.org/10.14359/18499
34. CEB-FIP (2011) Model code 2010. Document Competence Center Siegmar Kästl e.K, Germany
35. Bamforth P, Chisholm D, Gibbs J, Harrison T (2008) Properties of concrete for use in Eurocode 2
36. Arioglu N, Canan Girgin Z, Arioglu E (2006) Evaluation of ratio between splitting tensile strength and compressive strength for concretes up to 120 MPa and its application in strength criterion. ACI Mater J 103:18–24. https://doi.org/10.14359/15123
37. Azenha M, Sfikas IP, Wyrzykowski M, et al (2018) Chapter 6 temperature control. In: Fairbairn EMR, Azenha M (eds) Thermal cracking of massive concrete structures: state of the art report of the RILEM technical committee 254-CMS. Springer, pp 153–180
38. Klausen ABE (2017) Early age crack assessment of concrete structures. Norwegian University of Science and Technology
39. Wei Y, Liang S, Guo W, Hansen W (2017) Stress prediction in very early-age concrete subject to restraint under varying temperature histories. Cem Concr Compos 83:45–56. https://doi.org/10.1016/j.cemconcomp.2017.07.006
40. Neville AM, Brooks JJ (1987) Concrete technology. England: Longman Scientific & Technical
41. Mander JB, Priestley MJN, Park R (1989) Theoretical stress-strain model for confined concrete. J Struct Eng 114:1804–1826
42. Lee J, Fenves GL (1998) Plastic-damage model for cyclic loading of concrete structures. J Eng Mech 124:892–900. https://doi.org/10.1061/(asce)0733-9399(1998)124:8(892)
43. Honorio T, Bary B, Benboudjema F (2016) Multiscale estimation of ageing viscoelastic properties of cement-based materials: a combined analytical and numerical approach to estimate the behaviour at early age. Cem Concr Res 85:137–155. https://doi.org/10.1016/j.cemconres.2016.03.010
44. Bažant ZP, Baweja S (2000) Creep and shrinkage prediction model for analysis and design of concrete structures: Model B3. ACI Spec Publ SP-194:1–83
45. Wei Y, Hansen W (2013) Tensile creep behavior of concrete subject to constant restraint at very early ages. J Mater Civ Eng 25:1277–1284. https://doi.org/10.1061/(asce)mt.1943-5533.0000671
46. Bažant ZP, Baweja S (1996) Short form of creep and shrinkage prediction model B3 for structures of medium sensitivity. Mater Struct 29:587–593. https://doi.org/10.1007/bf02485965
47. Nguyen DH, Nguyen VT, Lura P, Dao VTN (2019) Temperature-stress testing machine - a state-of-the-art design and its unique applications in concrete research. Cem Concr Compos 102:28–38. https://doi.org/10.1016/j.cemconcomp.2019.04.019
48. Standards Australia (2018) AS3600-2018: Concrete structures. Standards Australia Limited, Sydney